CrossMark

AFSTI
Empowering food professionals

ORIGINAL ARTICLE

Development of chitosan based optimized edible coating for tomato (*Solanum lycopersicum*) and its characterization

Sanjib K. Paul[1] · Sudipto Sarkar[1] · Laxmi Narayan Sethi[1] · Sujit K. Ghosh[2]

Abstract In the present work experiments were carried out to optimize coating formulation in central composite rotatable design varying chitosan and glycerol concentration from 0.5 to 3% (w/w) and 0 to 3% (w/w) respectively as two independent factors. Total color difference and respiration rate was selected for tomato parameters and water vapor permeability and percentage solubility was selected for coating parameters as response. Quadratic polynomial models generated was adequate to explain the effects of the chitosan and glycerol concentrations on response variables. Experimental validation confirmed the adequacy of the coating formulation for tomato optimized by response surface methodology with 2.15% chitosan and 0.50% glycerol. Characterization of the optimized coating was undertaken in scanning electron microscope, X-ray diffraction (XRD) and Fourier transform infra-red (FTIR) spectroscopy. Microstructure image revealed proper continuity, integrity and surface micro structure of the developed coating. XRD and FTIR spectra revealed the pattern of ideal chitosan based coatings and also unfolded various crystallographic, structural and molecular involvement and couplings in coating properties. XRD pattern reflected semicrystalline structure of chitosan based developed edible coating having crystal form-1 and crystal form-II. In addition to other expected ideal peaks, FTIR also confirmed the presence of water in the coating. Residual acetic acid (solvent for coating formulation) is also evident at around 1700 cm^{-1} of FTIR spectra, corresponding to carbonyl vibration of the carboxylic acid.

Keywords Edible coating · Tomato · Microstructure · Crystallinity · FTIR · Optimisation

✉ Sanjib K. Paul
  sankumarpaul@gmail.com

[1] Department of Agricultural Engineering, Assam University, Silchar, Assam 788011, India

[2] Department of Chemistry, Assam University, Silchar, Assam 788011, India

Introduction

Tomato (*Lycopersicon esculentum* Mill) is a rich source of different nutrients and antioxidants, which produces huge health benefits to the consumers. Tomato is consumed or utilized in a diversified ways including raw, cooked, in the form of various processed products and also as an ingredient of various food products and drink formulations. Though it has huge potential in the production of various food products and also nutritional value but due to high moisture content, soft texture and high respiration rate it becomes highly perishable by mechanical, microbial and biochemical degradation, leading to the wastage of its significant fraction before it reaches to the consumer level (Kader 2002). Similar picture can be observed in case of other perishable fruits and vegetables in most of the developing countries. In addition to that existing chemical and synthetic product based storage and preservation technologies are becoming a global threat for environment as well as human health. Thus, a great need of research in the domain of alternative post harvest management technique is realized to reduce microbial and biochemical degradation and extension of shelf-life of tomato that can be effectively applied into other climacteric fruits and vegetables to reduce the postharvest losses and more

precisely contributing in the economy of the country. In this regard, edible-coating may be one the most suitable alternative to address all the above mentioned challenges.

Edible coatings and films are generally produced from renewable natural and biodegradable polymeric materials such as polysaccharides, proteins, lipids, or the combination of these components (composite and conglomerate coating/film). For the past 10 years, research on edible films and coatings in foods is driven due to the high demand of consumers for longer shelf-life and better quality of fresh foods as well as of environmentally and health friendly packaging. Thus, there is urgent need to select and develop a proper edible coating to prevents the growth of micro organisms, reduce physiological degradation of fresh produce.

Among different film-forming polysaccharides, chitosan is a highly non-toxic polysaccharide having excellent antimicrobial properties. It has been successfully used as a food wrap or coating because of its filmogenic properties, biocompatibility and biodegradability (Majeti and Ravi 2000; Singh et al. 2015).

Appropriate optimization of composition of edible coating followed by standardized coating process may contribute allot in solving the existing technological gap. Optimization process should include critical factors of both coated produce and coating itself. Though different researchers have applied chitosan in various fruits and vegetables like strawberry, citrus, banana, grapes, carambola and grape fruits to achieve certain goals (Gol et al. 2015; Malmiri et al. 2011), but the effect of plasticizer composition with chitosan on climacteric fruits, especially tomato during storage has rarely been analyzed till now. Some of the literatures revealed the optimum composition of different polysaccharide based coatings or film but the optimization criteria cannot be considered universal as they only emphasized on coated fruit parameters and excluded the coating characteristics. Viewing upon this fact, in the present work, an attempt has been made to optimize the chitosan based edible coating by studying its effect on various critical parameters of tomato and the coated film to control the deteriorative process. Further, it was also aimed to select appropriate model for optimization and experimental validation. To ensure the sustainability of the optimized and experimentally validated coating, it was further characterized by investigating its micro and submicro level structural features by using non-destructive techniques.

## Materials and methods

Materials

Tomatoes (*Solanum lycopersicum*) were grown in Silchar, Cachar (Assam) from the seeds of the *Shivam-F1 variety* (Century seeds Pvt. Ltd., New Delhi) and experimental sampling was done based on same maturity, ripening stage (Stage-2 i.e., Pink stage), uniformity in appearance (weight, size, shape and color) and free from any defect. Average tomato weight, locules number, pericarp thickness and fruit density of the sampled tomato were 62.0 ± 1.3 g, 2.6 ± 0.23, 7.12 ± 0.21 mm and 0.991 ± 0.001 g cm^{-3} respectively. They were then disinfected with sodium hypochlorite (0.01% v/v), washed and allowed to air-dry.

Chitosan is selected as coating material due to its non toxicity, microbial inhibiting activity and its suitability in the formation of coating and film. Chitosan (medium molecular weight), glycerol (87%) and other chemicals and reagents are of analytical grade and all are from Hi-media (Mumbai) and Merck (Germany) make. All glassware's used are sterilisable and borosilicate.

Experimental design for optimum coating formulation

Two factor central composite rotatable design (CCRD) was adopted for conducting the experiments and formulation of coating/film solutions. In the design chitosan and glycerol concentrations (% w/w) were taken as independent variables. Various fruit parameters and coating parameters were taken as response variables for the experimentation. Respiration rate (mg CO$_2$/kg h) and color difference (ΔE) were included as coated fruit parameters. Water solubility (%) and water vapor permeability or WVP (g/cm s Pa) were included as coated film parameters. One center point with six replications was used in this design to calculate the repeatability of the method (Mirhosseini et al. 2009). In the experimentation, concentration of chitosan and glycerol was varied from 0.5 to 3% (w/w) and 0 to 3% (w/w) respectively (Fig. 1). Experimental design revealed six replications of centre points at 1.75% (w/w) of chitosan and 1.5% (w/w) of glycerol concentration in the coating formulation. In these range fourteen combinations of edible coating/film formulations were prepared by dissolving them in 100 mL of 0.5% glacial acetic acid and stirred overnight. The set of combinations of independent variables of CCRD is represented in electronic supplementary material (ESM Table 1). The pH of the solutions was adjusted to pH 5.6 with 0.1 M sodium hydroxide and the solution was sieved through a mesh of 50 μm pore size. Sample tomatoes were dipped into the prepared coating

Fig. 1 Response surface plot for **a** total color difference and **b** respiration rate of coated tomato, **c** water vapor permeability (WVP) and **d** water solubility (%) of the coated film as a function of the concentrations of chitosan and glycerol in coating formulation
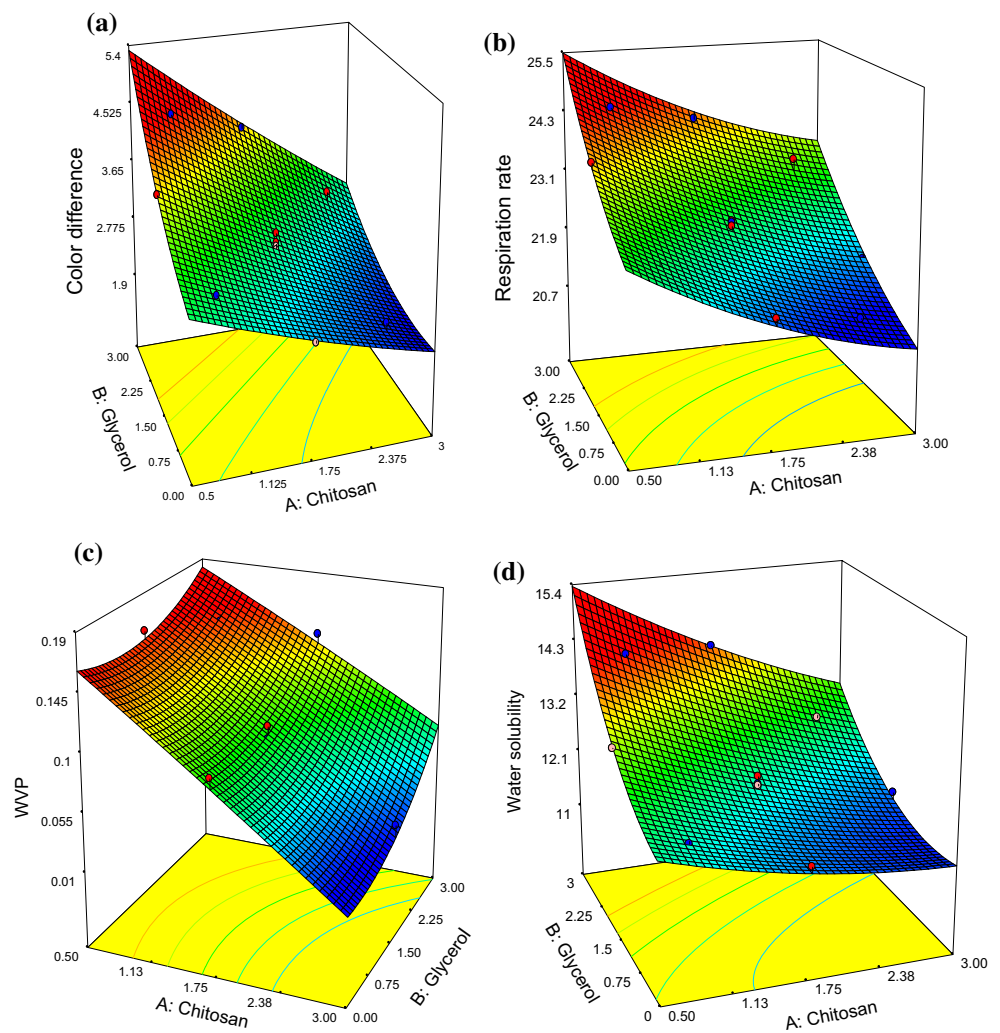
formulation for 1 min with 30 s of air drying time having 20 repeating cycles in a programmable dip coating machine (Xdip-MV1, Apex Instrument, Kolkata). Uncoated tomatoes as control samples were immersed in a 0.5% glacial acetic acid solution at pH 5.6 for the same duration of time. The treated and control tomato samples were dried in ambient conditions (30 ± 2 °C and 50–60% relative humidity) for 24 h. After setting a thin layer of edible coating on the surface of treated samples, control and coated tomatoes were stored at ambient conditions in the laboratory for further analysis.

Film of same thickness as applied on tomato surface was produced by casting appropriate volume (30–40 mL) for each combination of coating formulation on a plate of 9 cm diameter and subsequent drying at 40 °C for 48 h and then peeled off for further analysis.

Analysis of coated tomato and film for optimization of coating formulation

The effect of edible coatings having the constituents at different proportions on various response parameters were used to optimise the coating formulation. Respiration rate and colour parameters of tomato (ΔE) were determined just after coating (0th day) and on the 10th day of storage. Water vapour permeability (WVP) and solubility of the coated film were assessed on the 10th day of storage. Period of storage for the analysis was decided based on the shelf-life of control tomato. Initiation of visible spoilage symptoms on the stored samples was considered as the end point of the storage for optimisation (Malmiri et al. 2011).

Color change

Evaluation of the changes in color of the peel of both coated and control tomato samples were determined using a Hunter Lab Color Quest (Model Ultrascan Vis-Model,

USA). The results of color values were expressed in *L, a, b* system. The total color difference (*ΔE*) was calculated as the root mean square of the differences in individual *L, a* and *b* values (Maftoonazad and Ramaswamy 2005).

$$\Delta E = \left(\Delta L^2 + \Delta a^2 + \Delta b^2\right)^{0.5}$$

where *ΔL, Δa* and *Δb* were obtained as differences in *L, a* and *b* values of coated tomatoes on day 10 and day 0, thus representing the time related changes.

Respiration rate (RR)

Respiration rate of coated and control tomatoes were determined by following the method of AOAC (1992).

Water vapor permeability (WVP)

WVP of the coating was determined by the method described by García et al. (1998) for strawberry, but with slight modification. The coated tomatoes were placed in individual sample cups and equilibrated for 24 h in a desiccator chamber maintained at 98.2% RH with a $K_2Cr_2O_7$ saturated solution at 25 ± 4 °C. Water activity (a_w) of internal tissue of coated tomato was measured in a digital water activity meter (Hygrolab C1, Rotronic Instrument Corp-USA). The samples were weighed in an analytical balance and placed in an incubator equilibrated at 33.3% RH with $MgCl_2 \cdot 6H_2O$ at 25 °C. The samples were weighed at regular intervals to calculate weight loss with time. Data of weight loss were obtained for a period of 3 h. It was assumed that during the period of 3 h, loss of water was produced in conditions where water surface concentration remained constant and coincided with the equilibrium value $a_w = 0.988$ as equilibrated earlier. A control test with uncoated sample was also carried out to determine the mass transfer coefficient of water vapor in air (K_{air}) (Garcia et al. 2000).

Water vapor flux, *FI* (g cm^{-2} s^{-1}), was calculated from the slope of the weight loss versus time curves (*Dw/Dt*).The mass transfer area (*A*) was considered as the average surface area of the coated tomato. Surface area of the coated tomato was determined by volume to thickness ratio of the coating. As the coating was very thin, the effect of coating thickness in this method was non-significant. The mass transfer area (*A*) determined was verified by the adhesive tape method reported by Clayton et al. (1995).

$$FI = \frac{Dw}{Dt \cdot A}$$

Coating permeance, *p* (g m^{-2} s^{-1} Pa^{-1}), was determined using the following equation proposed by Garcia et al. (1998) for edible coatings:

$$FI = \frac{p_i - p_a}{\frac{1}{P} + \frac{1}{K_{air}}}$$

where p_i is the partial water vapor pressure corresponding to the tomato-coating interface. This was calculated considering the a_w of the tomato and the total water vapor pressure at 20 °C, p_a is the partial water vapor pressure in the environment with 33.3% relative humidity at 20 °C, and K_{air} is the mass transfer coefficient of water vapor in air.

The equation of Garcia et al. (1998) considers series transmission of water vapor flux through the coating and the surrounding air from the stomatal openings and membrane transmission pumps of the tomato skin.

WVP was calculated as: WVP = *Pd* where *d* is the coating thickness (cm). The whole experiment was performed at least five times for each coating type.

Percentage solubility

Solubility of coating in water was determined according to the method reported by Gontard et al. (1994). It was defined by the content of dry matter solubilized after 24 h immersion in water. The initial dry matter content of each peeled coating/film was determined by drying it to constant weight in an oven at 105 °C. Two disks of film (2 cm diameter) were cut, weighed, and immersed in 50 mL of water. After 24 h of immersion at room temperature with occasional agitation, the pieces of film were taken out and dried to constant weight in an oven at 105 °C, to determine the weight of dry matter which was not solubilized in water. The variation coefficient obtained between the three replicates made for each experiment was expressed as percentage solubility.

Model fitting and optimization of coating formulation

A generalized polynomial equation was used to relate the responses. Respiration rate (Y_1) and color difference (Y_2) as coated tomato parameters, whereas water solubility (Y_3) and water vapor permeability or WVP (Y_4) of coated film as coating parameter was individually correlated with the independent variables as follow:

$$Y_i = a_0 + a_1X_1 + a_2X_2 + a_{11}X_1^2 + a_{22}X_2^2 + a_{12}X_1X_2$$

where Y_i represents the response variables, a_0 is a constant, a_i, a_{ii} and a_{ij} are the linear, quadratic and interactive coefficients, respectively. The coefficients of the quadratic polynomial equations were calculated using experimental data. Model analysis, lack-of fit test and coefficient of determination (R^2) analysis were performed to determine the adequacy of the model. For any terms of independent

variables in the models, a large F-value and a small p value would show a more significant effect on the particular response variables. The terms statistically found non-significant were dropped from the initial models and experimental data were refitted only to significant ($p < 0.05$) independent variable effects in order to obtain the final reduced model (Mirhosseini et al. 2009; Singh et al. 2015).

Both numerical and graphical optimizations were performed to determine the optimum concentrations of independent variables (chitosan and glycerol) to achieve more desirable response. Respiration rate (mg CO_2/kg h), color difference (ΔE), water solubility (%) and water vapor permeability or WVP (g/cm s Pa) were considered as response parameters for optimization. Response variables were selected considering the critical quality parameters of both tomato and coated film, so that overall desirability can be achieved. Lower values (towards minimum) of all four responses were considered desirable for the optimization process. Considering the vital influence of all four responses on the quality attributes and shelf-life of tomato, as well as coating properties, equal importance or weighting co-efficient (1.0) is given to all the response parameters during the process of optimization. Three dimensional response surface plots were generated from the fitted models for each response to better visualize the interaction effects of chitosan and glycerol concentrations on the dependant parameters following the process as described by Singh et al. (2015). A numerical optimization was performed by the response optimizer for determining the exact optimum concentrations of independent variables leading to the overall optimum condition.

Experimental validation

Verification experiments were performed at the optimum concentrations of the chitosan and glycerol, and the experimental values of studied responses were compared with predicted response values by Duncans multiple range test. It is performed to verify the adequacy of the final response models developed during optimization. The optimization and comparison procedures were carried out using 'Design Expert-8' software.

Characterization of optimized coating

Experimentally validated optimized edible coating was further analyzed for their various morphological, structural and spectral properties to ensure its sustainability by investigating its micro and sub-micro level characteristics by different analytical techniques including SEM, XRD and FTIR without altering the constituents and characteristic features of the coating sample.

Surface integrity and microstructure of the coating

Surface integrity and coating microstructure of developed coating was observed by peeling off 3 cm² coated film from the surface of tomato. The coated film was dried at 35 °C under vacuum to remove the unbound moisture without disturbing the morphological and structural orientation of the coated film. The dried film was observed under scanning electron microscope (SEM, JEOL 6993V), operating at an acceleration voltage of 15 kV. Magnifications taken were 1500–4000× and the surface characteristics and morphological features of the coatings were observed.

X-ray difractrometry

Wide angle X-ray diffractograms were obtained with an X-ray diffractometer (Rigaku Miniflex). The XRD patterns were evaluated according to Zobel (1964).

Measurements were conducted in Bragg–Bretano (θ–2θ) symmetric geometry from 3° to 35° at steps of 0.01 degree and a time step of 100 s, and 45 kV and 40 mA were used for the tube power. Other parameters viz. percentage crystallinity and crystal characteristics were determined according to Singh et al. (2006).

FTIR spectroscopy

The Infra-red spectrum for the sample was obtained on a FTIR spectrometer (Nicolet Instruments 410 FTIR equipped with KBr optics and a DTGS detector) using KBr disc. The equipment was operated with a resolution of 2.0 cm⁻¹ and scanning range of 4000–370 cm⁻¹. The FTIR spectrum was analyzed using online spectroscopic analysis.

Statistical analysis

All the analytical experiments were carried out in triplicates ($n = 3$). Mean and Standard deviation (SD) were evaluated for all parameters and represented.

Model analysis, lack-of fit test and coefficient of determination (R^2) analysis were performed to determine the adequacy of the model. The terms statistically found non-significant were dropped from the initial models and experimental data were refitted only to significant ($p < 0.05$) independent variable effects in order to obtain the final reduced model.

Comparison of means of each dependent parameter was made (wherever needed) using Duncan's multiple range test at $p \leq 0.05$.

All the analysis of experimental design, model fitting and optimization in response surface methodology (RSM) is carried out by using Design Expert-8 statistical software

(Stat Ease Inc, USA). Remaining comparative analyses were carried out by using IBM SPSS Statics-19.0 software (Armonk, NY:IBM Corp).

Results and discussion

Effect of chitosan and glycerol concentration on response variables

Fourteen experiments were performed using CCRD for the two independent factors, viz., chitosan and glycerol concentration in coating formulation. The combinations of chitosan and glycerol in each formulation and the response values, viz., color difference, respiration rate, WVP and water solubility are graphically represented in Fig. 1. The response values for each corresponding combination of independent variables in CCRD are also provided as electronic supplementary material (ESM Table 1). The effects of variation in both the independent factors on various response parameters were used for numerical and graphical optimization in response surface methodology (RSM).

Effect on total color difference

Low O_2 and high CO_2 concentrations reduce the activities of various enzymes, including, those contributing in color changes. In Fig. 1a, it is very clear that the concentration of chitosan and glycerol has direct relationship with the total color difference (ΔE). The variation was found to be significant ($p \leq 0.01$) for both the independent parameters. It can be observed that higher concentration of chitosan and lower ($< 1\%$) concentration of glycerol has shown lower color deviation till the end of the experiment from its initial color of 0th day.

This result can be explained by the fact that attractive forces between chitosan molecules (cohesion) increase by increasing the chitosan concentration in edible coating formulation but higher concentrations of glycerol as plasticizer seems to reduce intermolecular forces along the chitosan chains, thus, increasing free volume, chain movements and finally, increase the permeability of chitosan based coating (Olivas and Barbosa-Canovas 2005). That might have allowed the moisture loss and gas exchange through the peel aperture leading to favorable conditions for the activity of chlorophyllase, polyphenol oxidase and peroxidase inside the tomato tissues, which might resulted in more change in surface color. Result of present study is in agreement with the findings of Zhang and Quantick (1997). These authors found that edible coatings changed internal atmosphere of banana and litchi, and strongly delayed color changes of coated fruits.

Effect on respiration rate

Figure 1b also revealed the similar pattern as in the case of total color difference. Lower respiration rate was observed at higher chitosan and lower glycerol concentration. This may be due to the formation of thick and continuous film that covered the epidermal openings, and modified the internal atmosphere with higher CO_2 and lower O_2 concentration (Garcia et al. 2010). The complete coverage of the surface stomata and a good cross linking with glycerol occurred probably when the chitosan content in the coating solution was increased to around 2.0%. Hence, the increase in chitosan content beyond 2.0% in the coating solution did not vary the respiration rate of tomatoes significantly. The respiration rate of coated tomatoes was significantly low when the coating solution contained 0.5% glycerol (Fig. 1b). Higher concentrations of glycerol as plasticizer reduces intermolecular forces along the polysaccharide chains, which increases the permeability of the coating (Malmiri et al. 2011). ANOVA data of respiration rate for the quadratic polynomial model (Table 1) revealed that main effects of chitosan and glycerol concentration have significant ($p \leq 0.01$) contribution over controlling the respiration rate. Data also revealed that the interaction effect of the independent parameters is non-significant over respiration rate of coated tomatoes. Previous works with various fruits including apple, strawberry, avocado, grapes, sweet cherry etc. showed similar outcome with coating materials such as carrageenan, whey protein, chitosan–oleic acid etc. (Maftoonazad and Ramaswamy 2005).

Effect on water vapor permeability (WVP)

It is clearly observed, at low concentrations of glycerol with an increase in the concentration of chitosan decreased the WVP (Fig. 1c). The higher glycerol content probably increases the WVP due to two reasons: (1) hydroxyl group on each carbon atom of glycerol binds with hydrogen in water leading to the transmission of water molecules through the coating, and (2) installation of glycerol molecules inside the polysaccharide network increases the intermolecular spacing in the coating matrix leading to the entry of water. It is further observed that in absence of glycerol results in the formation of crystalline and brittle films by polysaccharides, leading to the formation of pores and cracks in the coating, which resulted in higher WVP (Noel et al. 1992). ANOVA results revealed (Table 1) that the main effect of chitosan and glycerol concentration is highly significant ($p \leq 0.01$) on WVP, whereas, their interaction effects are non-significant in the fitted model. The results are in agreement with the findings of the previous works on the films and coatings made up of various hydrophilic substances including starch, carrageenan and

Table 1 Analysis of variance (ANOVA) of response surface quadratic model for total color difference (ΔE), respiration rate, water vapor permeability (WVP) and water solubility (%)

Source	ΔE		Respiration rate		WVP		% Water solubility	
	F value	p value	F value	p value	F value	p value	F value	p value
Model	101.53***	< 0.0001	83.04***	< 0.0001	42.40***	< 0.0001	151.57***	< 0.0001
X_1-chitosan	267.04***	< 0.0001	145.77***	< 0.0001	183.01***	< 0.0001	232.85***	< 0.0001
X_2-glycerol	216.66***	< 0.0001	259.84***	< 0.0001	20.33***	0.0028	457.48***	< 0.0001
X_1X_2	10.52**	0.0142	0.043	0.8421	1.20	0.3101	12.02**	0.0104
X_1^2	0.61	0.4614	4.85*	0.0635	0.047	0.8348	4.78*	0.0650
X_2^2	13.33***	0.0082	5.93**	0.0450	7.13**	0.0320	53.96***	0.0002

***Significant at 1% level, **significant at 5% level, *significant at 10% level

chitosan with or without plasticizers like glycerol and sorbitol (Henrique et al. 2007; Laohakunjit and Noomhorm 2004).

Effect on water solubility (%)

Changes in water solubility (%) with variation in concentrations of chitosan and glycerol are shown in Fig. 1d. Lower concentration of glycerol with higher fraction of chitosan demonstrated lower percentage solubility. It was observed from ANOVA (Table 1) that main linear effect of both the independent variables ($p \leq 0.01$), as well as their interaction ($p \leq 0.05$) and quadratic effects ($p \leq 0.1$) were significant on controlling water solubility of the coating. This can be justified with the fact that the formation of sufficient inter-molecular hydrogen cross linkages between chitosan, glycerol and/or water molecules in the coating matrix at lower to moderate concentration of glycerol in the formulation with sufficient chitosan during the gel processing stage reduced the solubility of the coated film (Salmieri and Lacroix 2006). On the other hand, higher solubility was observed in those films produced with formulation having higher fraction of glycerol with lower concentration of chitosan. Increase in the concentration of both the constituents might have contributed significantly in raising the hydrophilic-hydrophobic ratio resulting in the progressive increment in solubility (Bourtomm 2008).

Model fitting and optimization of coating formulation

Monitoring of the changes in quality attributes of tomato revealed that the control tomatoes showed initial deteriorating symptoms at day 10 of storage under ambient conditions. Total color difference and respiration rate of uncoated (control) tomatoes were 3.66 ± 0.07 and 42.6 ± 0.98 mg CO_2/kg h respectively at day 10 of storage. The final reduced models were obtained using experimental data. The individual significance p value of independent variables and their interactions are shown in Table 1.

Table 2 reveals the predicted regression coefficients for the response variables, along with the corresponding R^2 and R^2 (adj). Results demonstrated that the generated quadratic polynomial models are adequate to explain the effects of the chitosan and glycerol concentrations on the response variables of coated tomato samples. Each studied response was evaluated as function of main, quadratic and interaction effects of chitosan and glycerol concentrations. Independent effect of chitosan (X_1) and glycerol concentration (X_2) had the most significant ($p < 0.01$) contribution on the responses as compared to the quadratic and interaction effects. The interaction effects of chitosan and glycerol had non-significant ($p > 0.1$) effect on respiration rate and WVP, but it is also be kept in the final reduced models since the other effects of chitosan and glycerol were significant ($p < 0.01$ or $p < 0.05$) for the same response (Malmiri et al. 2011). The final reduced models to predict total color difference and respiration rate of coated tomato and WVP, as well as water solubility of the same coated film as function of chitosan (X_1) and glycerol (X_2) concentrations are derived as:

$$\text{Color difference } (Y_1) = 2.94 - 0.62X_1 + 0.56X_2 - 0.17X_1X_2 + 0.032X_1^2 + 0.15X_2^2$$

$$\text{Respiration rate } (Y_2) = 22.48 - 0.72\ X_1 + 0.97X_2 - 0.018X_1X_2 + 0.14X_1^2 + 0.16X_2^2$$

$$\text{WVP } (Y_3) = 0.094 - 0.044X_1 + 0.015X_2 - 0.005X_1X_2 + 0.00075X_1^2 + 0.00925X_2^2$$

$$\text{Water solubility } (Y_4) = 12.11 - 0.61X_1 + 0.85X_2 - 0.20X_1X_2 + 0.093X_1^2 + 0.31X_2^2$$

For optimization, the effect of chitosan and glycerol concentration on total color difference and respiration rate

Table 2 Model coefficients, regression coefficients, R^2 and R^2 (adj) for the final reduced models

Model coefficients and regression coefficients	Total color difference	Respiration rate	Water vapor permeability	Water solubility
Model constant (a_0)	2.94	22.48	0.094	12.11
Linear coefficient (a_1)	− 0.62	− 0.72	− 0.044	− 0.61
Linear coefficient (a_2)	0.56	0.97	0.015	0.85
Quadratic coefficient (a_{11})	0.032	0.14	0.00075	0.093
Quadratic coefficient (a_{22})	0.15	0.16	0.00925	0.31
Interaction coefficient (a_{12})	− 0.17	− 0.018	− 0.005	− 0.20
R^2	0.9864	0.9834	0.9680	0.9908
R^2 (adj)	0.9767	0.9716	0.9452	0.9843

of coated tomato and WVP, as well as water solubility (%) of the same coated film was assayed on 10th day of coating. Based on desirable goal the independent parameters were optimized for minimum values of all the responses. The results of the analysis indicated that optimum concentration of chitosan and glycerol is 2.15 and 0.50%, respectively, within experimental ranges. The final reduced fitted model also predicted the value of total color difference and respiration rate of coated tomato as 2.34 and 21.42 mg CO_2/kg h, and WVP and water solubility (%) of the coated film as 0.067×10^{-11} g/cm s Pa and 11.41% respectively at the optimum concentration of coating formulation.

Experimental validation

Verification experiments were performed at the optimum concentration of the chitosan and glycerol (2.15 and 0.50% w/w respectively). All the dependent experimental parameters were analyzed in triplicates for the samples of 10th days of storage following the same process adopted during the optimization experiments. Experimental validation revealed the value of total color difference and respiration rate of coated tomato as 2.31 ± 0.01 and 21.21 ± 0.06 mg CO_2/kg h, whereas WVP and water solubility (%) of the coated film as $0.066 \pm 0.00 \times 10^{-11}$ g/cm s Pa and $11.54 \pm 0.04\%$ respectively at the optimum concentration of coating formulation. Comparison test demonstrated that there is no significant ($p > 0.05$) difference between predicted and experimental values for all response variables. Analysis of % residuals further revealed that predicted value of respiration rate and WVP is highly close with the experimental value with % residual of less than 1%. Overall color difference and water solubility also demonstrated very less % residuals (slightly higher than 1%) between their predicted and experimental values. The closeness between these values of responses validated the adequacy of final reduced models fitted by RSM.

Characterization of optimized coating

Surface integrity and microstructure of the coating

The SEM image of developed optimized coating indicates sufficient homogenization and uniform distribution of chitosan and glycerol blend (Fig. 2). Absence of distinct separation of different coating constituents, microphase separation and pores confirmed their proper and uniform blending. Integrity and continuity of the coating is also observed even at higher magnification of ×3000 (Fig. 2b). Absence of aggregation and ghost granules suggests
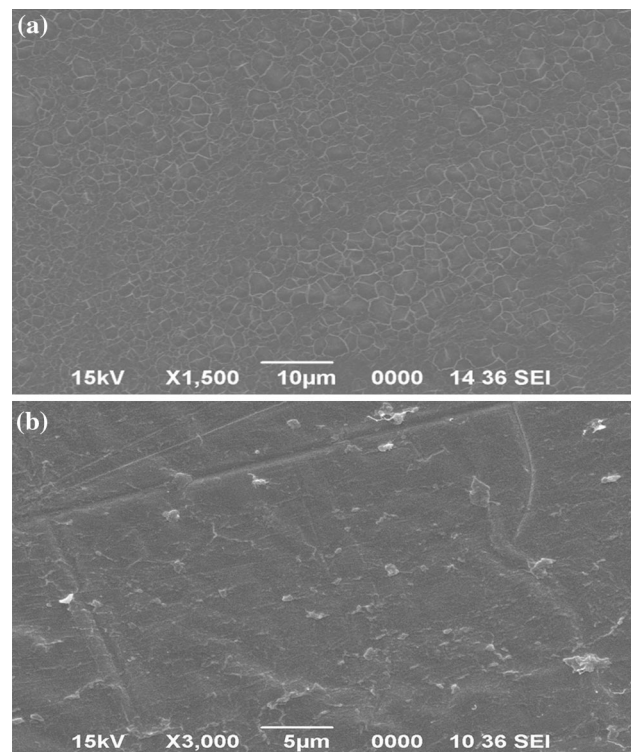

Fig. 2 Scanning electron microstructure (SEM) image for surface morphological analysis of the coating at different magnifications **a** X1500 and **b** X3000

adequate gel formation by sufficient stirring of the chitosan–glycerol formulation, which enabled proper mixing leading to the smoother surface with absence of any cracks at the microstructure level of the coating. It has been hypothesized that glycerol can enter into the network of the chitosan chain, where it disrupts the inter- and intramolecular hydrogen bonds and makes the polymer plastic with the formation of new hydrogen interactions, thereby forming a continuous phase of a plasticized coating (Jesús et al. 2014). Similar type of microstructure of starch based edible coating and film were also reported by various previous workers but they reported about the presence of ghost granules in their film and also suggested the addition of oil to render more homogeneity and smoother surface (Das et al. 2012; Nuthong 2011).

Continuity, integrity and surface microstructure of the coating suggests the uniform covering of the epidermal apertures of the tomato peel surface that effectively reduced the gas and water vapor exchange. This effect, further, contributed in reduction of respiration rate and WVP, leading to less color change during storage (Malmiri et al. 2011).

X-ray diffractometry

Figure 3 shows XRD pattern of optimized chitosan based edible coatings. In summary, chitosan and chitosan-derived networks usually exhibit semicrystalline structures due to the free-energy balance caused by hydrogen bond formation (Costa-Júnior et al. 2009). Souza et al. (2010) have shown that the residual reflection around $10°–15°$ (2θ) reflects the presence of the crystal form I and the strongest reflection at $2\theta = 20°–25°$ corresponds to the crystal form II. It is known that chitosan always contains bound water (around 5%) even if it is completely dried. The crystalline peak centered at around $10°$ (peak I) is attributed to the hydrated crystalline structure of chitosan and also the
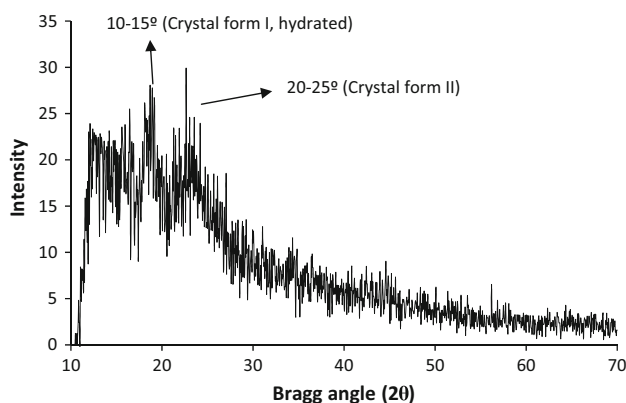
Fig. 3 X-ray diffraction (XRD) pattern of experimentally validated edible coating

presence of chain segments of chitin (Souza et al. 2010). Another peak registered near $20°$ (peak II) is reported to be the indication of the relatively regular crystal lattice in chitosan (Souza et al. 2010). The diffraction peak at around $20°–25°$ (2θ) observed in this work is in agreement with other published results (Ziani et al. 2008).

Comparison of the observed XRD pattern of optimized chitosan based edible coatings with previously disclosed pattern of neat chitosan based edible coatings (without plasticizer) as reported by Jesús et al. (2014) further revealed some other significant conclusions. It was observed that the introduction of glycerol in the coating resulted into reduction in intensity of diffractogram. This decrease indicates that the crystalline orientation of chitosan is disorganized during the processing of coating formulation. The presence of glycerol as plasticizer may have also contributed to this change by entering into polysaccharide network (Singh et al. 2009a). This might affected the inter-molecular and intra-molecular hydrogen bonds with newly formed chitosan–glycerol hydrogen bonds and disintegrated the packaging of the molecular chains of chitosan. Similar effect of glycerol was also previously reported in chitosan based (Jesús et al. 2014), as well as starch based edible films (Singh et al. 2009a).
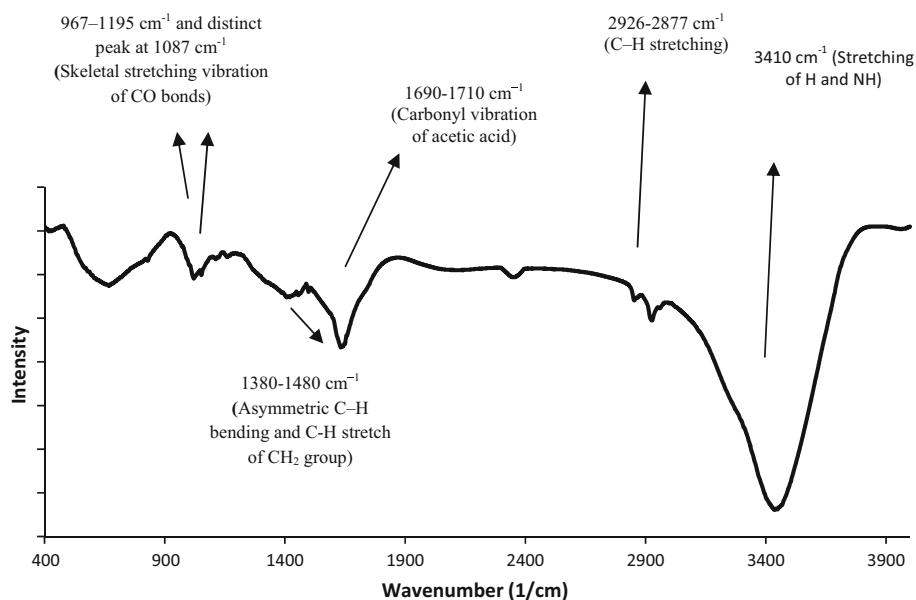
It was also reported that flexibility of the film is also proportionally affected by the crystallinity of the coating material (Souza et al. 2010). These structural variations might further lead to the differences in WVP, water solubility, O_2 and CO_2 permeability and various other previously discussed parameters of the coating.

FTIR spectroscopy

FTIR analysis was used to evaluate possible chemical interactions between the components of polymeric coating (Fig. 4). The spectrum of the developed coating was almost similar to previous reports for chitosan and chitosan based coating and films without plasticizer (Jesús et al. 2014; Xu et al. 2005). However, some deviation in absorption intensities were also observed as compared to the previously reported FTIR spectra of neat chitosan based edible films.

The IR spectrum showed the expected pattern with absorption peaks at nearby 3360 and 967–1195 cm^{-1}, which corresponds to stretching of OH and NH bonds and to stretching vibration of CO bonds, respectively (Pranoto et al. 2005). Absorption peaks at 2926 and 2877 cm^{-1} (C–H stretching), a band at 1600 cm^{-1} (bending amine groups (–NH$_2$) and also confirms the presence of water), 1480–1380 cm^{-1} (asymmetric C–H bending and C–H stretch of CH$_2$ group) and 1087 cm^{-1} (skeletal vibration involving the bridge C–O stretch) of glucosamine residue were also observed. This result is in agreement with the

Fig. 4 Fourier transform infrared spectroscopic (FTIR) spectra of experimentally validated edible coating

967–1195 cm⁻¹ and distinct peak at 1087 cm⁻¹ (Skeletal stretching vibration of CO bonds)

1690-1710 cm⁻¹ (Carbonyl vibration of acetic acid)

2926-2877 cm⁻¹ (C–H stretching)

3410 cm⁻¹ (Stretching of H and NH)

1380-1480 cm⁻¹ (Asymmetric C–H bending and C-H stretch of CH₂ group)

Intensity

Wavenumber (1/cm)

various previous reports including Jesús et al. (2014). The findings of this work further strengthened their previous observations about the effect of glycerol mainly in two major peaks at the 1660–1550 cm⁻¹ region (bending amine groups (–NH₂), and the strong band at around 1480–1380 cm⁻¹ (asymmetric C–H bending, C–H stretch of CH₂ group and also bending to the –OH) of the developed optimized edible coating. This can be explained by the fact that there could be an alteration of the arrangement in the coating matrix due to the interactions of the glycerol with the –OH and –NH groups in the polysaccharide. Similar effect of glycerol is also reported in edible films of various other biopolymers including, kidney bean starch (Singh et al. 2009a) and zein (Singh et al. 2009b).

In addition, the residual acetic acid is evident at around 1700 cm⁻¹, corresponding to carbonyl vibration of the carboxylic acid. This peak is a consequence of the low volatility of acid (Lawrie et al. 2007). Though, the intensity (shape and width) of the peaks recognize the vibrational attributes and the spread of vibrational frequencies, but the peak intensities and positions are only indicative of the degree of order and conformation in the system (Singh et al. 2009a). So, it is not the direct and conclusive technique for the purpose of crystallinity assessment.

Conclusion

Coating of tomatoes by chitosan based formulation with glycerol as plasticizer was found to effectively control various physiological parameters of tomato and hence, has the potential to increase the shelf-life. Composition of coating formulation was found to have direct relationship

with fruit parameters (respiration rate and *ΔE*) and coating parameters (WVP and % water solubility). SEM image revealed proper continuity, integrity and surface micro structure of the best identified coating. XRD and FTIR spectrum revealed the pattern of ideal chitosan based coatings and also unfolded various crystallographic, structural and molecular involvement and couplings in coating properties.

It is further expected that the effectiveness of the optimum coating formulation can probably be improved by the addition of certain functional additives for the enhancement of structural and functional properties with synergistic effects. Hence, this study strengthens the scope for further research in the domain of active and functional edible coating.

References

AOAC (1992) Official methods of analysis of the Association of Official Analytical Chemistry, 11th edn. Association of Official Analytical Chemists, Washington

Bourtomm T (2008) Edible films and coatings: characteristics and properties. Int Food Res J 15(3):1–12

Clayton M, Amos ND, Banks NH, Morton RH (1995) Estimation of apple fruit surface area. N Z J Crop Hortic Sci 23:345–349

Costa-Júnior ES, Barbosa-Stancioli EF, Mansur AAP, Wander LV, Herman SM (2009) Preparation and characterization of chitosan/ poly (vinyl alcohol) chemically crosslinked blends for biomedical applications. Carbohydr Polym 76:472–481

Das DK, Dutta H, Mahanta CL (2012) Development of a rice starch-based coating with antioxidant and microbe-barrier properties and study of its effect on tomatoes stored at room temperature. LWT Food Sci Technol 50:272–278

Garcia MA, Martino MN, Zaritzky NE (1998) Plasticized starch based coatings to improve strawberry (*Fragaria ananassa*) quality and stability. J Agric Food Chem 46:3758–3767

Garcia MA, Martino MN, Zaritzky NE (2000) Lipid addition to improve barrier properties of edible starch-based films and coatings. J Food Sci 65:941–947

Garcia LC, Pereira LM, Sarantópoulos CIGL, Hubinger MD (2010) Selection of an edible starch coating for minimally processed strawberry. Food Bioprocess Technol 3:834–842

Gol NB, Chaudhari ML, Rao TVR (2015) Effect of edible coatings on quality and shelf life of carambola (*Averrhoa carambola* L.) fruit during storage. J Food Sci Technol 52(1):78–91

Gontard N, Duchez C, Cuq JL, Guilbert S (1994) Edible composite films of wheat gluten and lipids: water vapour permeability and other physical properties. Int J Food Sci Technol 29(1):39–50

Henrique CM, Teófilo RF, Sabino L, Ferreira MMC, Cereda MP (2007) Classification of cassava starch films by physicochemical properties and water vapor permeability quantification by FTIR and PLS. J Food Sci 72:184–189

Jesús RR, Tomás JM, Dalia IS, Jaime L, Herlinda SV (2014) Chitosan/hydrophilic plasticizer-based films: preparation, physicochemical and antimicrobial properties. J Polym Environ 22:41–51

Kader AA (2002) Post-harvest technology of horticultural crops, 3rd edn. Agriculture and Natural Resources, University of California, Oakland, p 535

Laohakunjit N, Noomhorm A (2004) Effect of plasticizers on mechanical and barrier properties of rice starch film. Starch 56:348–356

Lawrie G, Keen I, Drew B, Chandler-Temple A, Rintoul L, Fredericks P, Grøndahl L (2007) Interactions between alginate and chitosan biopolymers characterized using FTIR and XPS. Biomacromolecules 8(8):2533–2541

Maftoonazad N, Ramaswamy HS (2005) Post harvest shelf-life extension of avocados using methyl cellulose-based coating. LWT Food Sci Technol 38:617–624

Majeti NV, Ravi K (2000) A review of chitin and chitosan applications. React Funct Polym 46:1–27

Malmiri HJ, Osman A, Tan CP, Abdul RR (2011) Development of an edible coating based on chitosan–glycerol to delay 'Berangan' banana (*Musa sapientum* cv. Berangan) ripening process. Int Food Res J 18:989–997

Mirhosseini H, Tan CP, Nazimah SAH, Salmah Y, Boo HC (2009) Characterization of the influence of main emulsion components on the physicochemical properties of orange beverage emulsion using response surface methodology. Food Hydrocoll 23(2):271–280

Noel TR, Ring SG, Whittman MA (1992) The structure and gelatinization of starch. Food Sci Technol Today 6:159–162

Nuthong P (2011) Visualization of oil droplet in rice starch film using confocal laser scanning microscope (CLSM). J Microsc Soc Thail 4:9–12

Olivas GI, Barbosa-Canovas GV (2005) Edible coatings for fresh-cut fruits. Crit Rev Food Sci Nutr 45:657–670

Pranoto Y, Rakshit SK, Salokhe VM (2005) Enhancing antimicrobial activity of chitosan films by incorporating garlic oil, potassium sorbate andnisin. LWT Food Sci Technol 38:859–865

Salmieri S, Lacroix M (2006) Physicochemical properties of alginate/polycaprolactone-based films containing essential oils. J Agric Food Chem 54:10205–10214

Singh V, Ali SZ, Somashekar R, Mukherjee PS (2006) Nature of crystallinity in native and acid modified starches. Int J Food Prop 9:845–854

Singh N, Belton PS, Dominique MRG (2009a) The effects of iodine on kidney bean starch: films and pasting properties. Int J Biol Macromol 45:116–119

Singh N, Dominique MRG, Belton P, Susan AB (2009b) Zein-iodine complex studied by FTIR spectroscopy and dielectric and dynamic rheometry in films and precipitates. J Agric Food Chem 57:4334–4341

Singh TP, Chatli MK, Sahoo J (2015) Development of chitosan based edible films: process optimization using response surface methodology. J Food Sci Technol 52(5):2530–2543

Souza BWS, Cerqueira MA, Martins JT, Casariego A, Teixeira JA, Vicente AA (2010) Influence of electric fields on the structure of chitosan edible coatings. Food Hydrocoll 24:330–335

Xu XY, Kim KM, Hanna MA, Nag D (2005) Chitosan–starch composite film: preparation and characterization. Ind Crop Prod 21:185–192

Zhang D, Quantick PC (1997) Effects of chitosan coating on enzymatic browning and decay during postharvest storage of litchi (*Litchi chinensis* Sonn.) fruit. Postharvest Biol Technol 12:195–202

Ziani K, Oses J, Coma V, Maté JI (2008) Effect of the presence of glycerol and Tween 20 on the chemical and physical properties of films based on chitosan with different degree of deacetylation. LWT Food Sci Technol 41:2159–2165

Zobel HF (1964) X-ray analysis of starch granules. In: Whistler RL (ed) Methods in carbohydrate chemistry, vol IV. Academic Press Inc., London